Fundamental Intrinsic Lifetimes in Semiconductor Self-Assembled Quantum Dots

Wen Xiong,[1] Xiulai Xu,[2] Jun-Wei Luo,[3,4,5,*] Ming Gong,[4,6,7,†] Shu-Shen Li,[3,4,5] and
Guang-Can Guo[4,6,7]

[1]*Department of Physics, Chongqing University, Chongqing 401331, China*

[2]*Beijing National Laboratory for Condensed Matter Physics, Institute of Physics, Chinese Academy of Sciences, Beijing 100190, China*

[3]*State Key Laboratory of Superlattices and Microstructures, Institute of Semiconductors, Chinese Academy of Sciences, Beijing 100083, China*

[4]*Synergetic Innovation Center of Quantum Information and Quantum Physics, University of Science and Technology of China, Hefei, Anhui 230026, China*

[5]*College of Materials Science and Opto-Electronic Technology, University of Chinese Academy of Sciences, Beijing 100049, China*

[6]*CAS Key Laboratory of Quantum Information, University of Science and Technology of China, Hefei 230026, China*

[7]*CAS Center For Excellence in Quantum Information and Quantum Physics, University of Science and Technology of China, Hefei 230026, China*

Self-assembled quantum dots (QDs) provide an ideal platform for realization of *on-demand* maximally entangled photon pairs, which is essential for quantum-information technologies. When the two intermediate exciton states are indistinguishable in energy, the biexciton cascade process naturally yields the maximally entangled photon pairs. However, because of the low symmetry of QDs, the two bright states should belong to different irreducible representations in realistic experiments, and their energy difference, called the "fine-structure splitting" (FSS), is much larger than their homogeneous broadening, giving rise to only classically correlated photon pairs by erasing the "which-way" information. In this work, we show that since these two states belong to different representations, their lifetimes should also be slightly different, which is termed "exciton lifetime asymmetry." In contrast to the extensively studied FSS, investigation of this lifetime asymmetry is missing in the literature. Here we conduct an investigation of the exciton lifetime asymmetry in self-assembled QDs and present a theory to deduce this asymmetry *indirectly* from measurable qualities of QDs. We further reveal that the intrinsic lifetimes and their asymmetries are more fundamental quantities of QDs, which determine the upper bound of the extrinsic lifetime asymmetries. Exact relations between lifetime asymmetries, FSS, and the polarization angle are also derived. These relations may be measured in experiments by studying the degree of polarization, as well its evolution under external stress. Our findings provide a complete description of the symmetry of the optical properties of QDs, which can give an important basis to deepen our understanding of QDs.

I. INTRODUCTION

Self-assembled quantum dots (QDs) provide a promising platform for realization of on-demand entangled photon pairs from the biexciton-exciton-vacuum cascade process [1], which are essential for practical quantum communication [2–7]. When the two intermediate exciton states are indistinguishable in energy [see Fig. 1(a)], the output photons construct the maximally entangled Bell state,

$$|\psi\rangle = \frac{1}{2}(|HH\rangle + |VV\rangle), \qquad (1)$$

*jwluo@semi.ac.cn

†gongm@ustc.edu.cn

where H and V define the polarization of the photon. However, in experiments, the major obstacle in realizing this goal comes from the nondegeneracy of the two intermediate bright exciton states, in which their energy difference, called "fine-structure splitting" (FSS), with typical magnitude of tens of microelectronvolts, is much larger than the homogeneous broadening of the emission lines ($\Gamma \sim 1\ \mu\mathrm{eV}$ [8–10]), and thus the "which-way" information is erased and only classically correlated photons instead of maximally entangled photon pairs can be created from this process. In the past decade, tremendous efforts have been devoted to eliminate this splitting by the application of all possible experimental techniques, including thermal annealing [11–15], use of an electric

field [16–23], use of a magnetic field [24–27], and external stress [28–38]. However, none of them are efficient. In experiments, the entangled photon pairs were demonstrated in a way that involved first picking out the QDs with small FSS from a QD ensemble after postannealing and then eliminating the FSS with use of magnetic fields [27]. During the tuning of FSS via an external magnetic field, it was found that not all the FSS in QDs can be tuned to zero. Because of this, only a tiny fraction of QDs grown even in the same conditions can be used to realize entangled photon pairs. Moreover, these devices can work only at low temperature since the emitted exciton energies are very close to the emissions from the wetting layer [39].

The mechanism underlying the difficulty in eliminating the FSS comes from the low symmetry of self-assembled QDs. It is impossible to restore the higher symmetry of the bulk materials in QDs by the aforementioned techniques [11–13,16–18,25–28]. This mechanism was first pointed out by Bester *et al.* [40,41], in which the strain effect (from lattice mismatch) and interface effect or the defects in realistic materials can lower the symmetry of QDs from the parent T_d symmetry to C_{2v} symmetry [42]; thus the macroscopic symmetry of QDs is not necessary the true symmetry of QDs. On the basis of this symmetry analysis, small or vanishing FSSs are expected to be found in QDs with relatively high symmetries [43]. In 2010, Singh *et al.* [44] found a lower bound of FSS is expected for a general QD, which prohibits the tuning of FSS to zero by external stress, as used in some experiments. To understand this effect, Gong *et al.* [45] proposed a minimal two-band model to uncover the reason why the FSS cannot be tuned to zero with a single external force for a general QD. This model contains two real numbers, and thus the FSS can be eliminated by two independent external forces [46]. This tunablility should be independent of the wavelength of QDs, and thus entangled pairs well below the wetting layer can be realized, which has the potential to realize on-demand entangled photon pairs of any wavelength. By use of three external forces, it is possible to construct a wavelength-tunable entangled photon emitter [47–49], opening the door for interfacing between QDs and other solid-state systems and even between dissimilar QDs. This proposal was recently realized in experiments [50–54] in self-assembled InAs/GaAs QDs, in which the wavelength of the exciton can be tuned in the range of several millielectronvolts.

From the symmetry point of view, since the two bright exciton states belong to two different representations for QDs with C_{2v} symmetry [55] [see the corresponding symmetry table in Fig. 1(b)], they should have not only different energies but also different lifetimes. The lifetime difference between two bright exciton states is termed "exciton lifetime asymmetry" [see Fig. 1(a)]. In contrast to the extensively studied FSS, investigation of this anisotropy effect is missing in the literature. In this
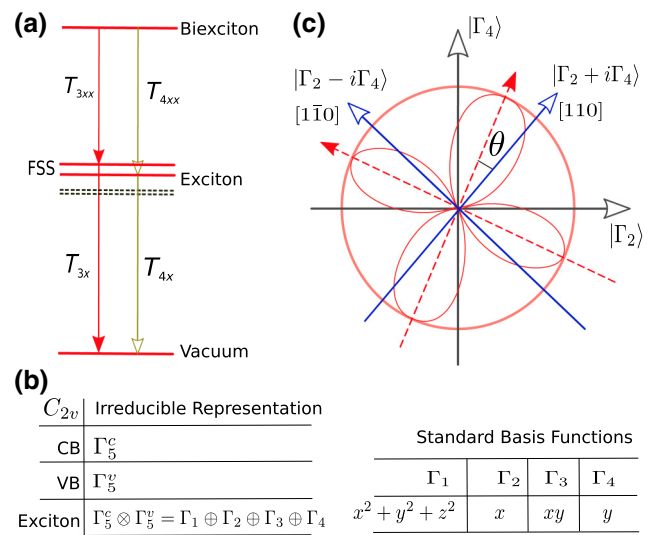

FIG. 1.   Direct consequence of low symmetry in QDs. (a) The two exciton bright states (solid lines) have different energies and lifetimes when they belong to different irreducible representations. (b) The basic irreducible representations of the conduction band (CB), valence band (VB) and the exciton, and their basis for QDs with C_{2v} symmetry. (c) In the presence of weak C_1 potential, direct coupling between the two bright states leads to wave-function mixing, and thus the emission will deviate from the [110] and [1$\bar{1}$0] directions.

work, we conduct an investigation of the exciton lifetime asymmetry in self-assembled QDs and present a theory to deduce lifetime asymmetry *indirectly* from measurable qualities of QDs. We further reveal that the intrinsic lifetime and the asymmetries are more fundamental quantities of QDs and unravel some exact relations between FSS, polarization angle, and lifetime asymmetries for excitons and biexcitons in QDs. Methods to measure these lifetimes are also proposed. These exact relations are verified by our performing atomistic simulations of self-assembled QDs using the empirical pseudopotential method [56,57].

II. ATOMISTIC SIMULATION METHOD

We use the empirical pseudopotential method [56,57] to simulate the electronic and optical properties of self-assembled QDs. In this calculation, we model (In,Ga)As/GaAs QDs by embedding them in a much larger GaAs supercell with periodic boundary conditions and minimize the total strain energy using the valence-force-field model [58,59]. The single-particle wave functions are determined by

$$\left[-\frac{1}{2}\nabla^2 + V_{\text{ps}}(\mathbf{r}) \right] \psi_i = E_i \psi_i, \qquad (2)$$

where i is the site index and $V_{\text{ps}}(\mathbf{r}) = \mathcal{V}_{\text{soc}}(\mathbf{r}) + \sum_{i\alpha} \mathcal{V}_{i\alpha}(\mathbf{r} - \mathbf{R}_{i\alpha})$ is the empirical pseudopotential, where

$\mathbf{R}_{i\alpha}$ is the position of atom type α and $\mathcal{V}_{soc}$ is the spin-orbit-coupling term. The position of each atom in the supercell is obtained by minimization of the total strain energy. The exciton and biexciton energies are then calculated by use of the configuration-interaction method taking into account the Coulomb interaction and exchange-correlation interaction [56,57,60]. The deformation of positions $\mathbf{R}_{i\alpha}$ accounts for the symmetry lowering from T_d to C_{2v} in realistic QDs.

III. THEORETICAL MODELING

We conduct the symmetry analysis of QDs as given in Ref. [45] by decomposing the QD Hamiltonian H into two parts: $H = H_{2v} + V_1$, where H_{2v} is a predominant term having C_{2v} symmetry and includes the kinetic energy, Coulomb interaction, and all potentials with C_{2v} symmetry; and V_1, which represents the remaining potentials lowering the symmetry of QDs from C_{2v} to C_1. The V_1 potential can be treated as a perturbation to H_{2v} considering its weak effect on the energy levels of QDs. The two bright states of H_{2v} are denoted as $|3\rangle = |\Gamma_2 - i\Gamma_4\rangle$ and $|4\rangle = |\Gamma_2 + i\Gamma_4\rangle$, respectively, where $|\Gamma_i\rangle$ ($i = 1, 2, 3, 4$) are the irreducible representations of the C_{2v} point group [see Fig. 1(b) and 1(c) and the symmetry table in Ref. [55]]. We consider quantities of the H_{2v} Hamiltonian to be intrinsic. Our key idea is that since these two bright exciton states belong to two different irreducible representations, they must have different energies with an energy separation of FSS, and different lifetimes ($\tau_{3\eta}$ and $\tau_{4\eta}$, respectively) with a time difference termed "intrinsic lifetime asymmetry" $\delta\tau_\eta$. Hence, $\tau_{3\eta} = \tau_\eta + \delta\tau_\eta/2$ and $\tau_{4\eta} = \tau_\eta - \delta\tau_\eta/2$, where τ_η is the averaged lifetime (hereafter $\eta = x$ for an exciton and $\eta = xx$ for a biexciton). Since the V_1 potential is inevitable and uncontrollable in experiments, the intrinsic lifetimes and their asymmetries cannot be measured *directly* in experiments.

To simplify the effective model for the total Hamiltonian H, we take advantage of two additional features. Firstly, the time-reversal symmetry for an exciton, $\mathcal{T}^2 = +1$ (excitons have integer spins), ensures that the wave functions of the two bright exciton states can be made real simultaneously [61]. Secondly, the spin selection rule and the large energy difference between the dark and bright states (typically about 0.2–0.5 meV [62]) forbid the mixing of dark states ($m = \pm 2$) and bright states ($m = \pm 1$) even in the presence of the V_1 term. The dark exciton states can be probed only by coupling to bright states through in-plane external magnetic fields [25–27]. We can thus safely ignore the dark states and construct the effective model on the basis of only the two bright exciton states of H_{2v}, as follows:

$$H = E_0 + \delta\sigma_z + \kappa\sigma_x, \tag{3}$$

where E_0 is the mean energy of two bright exciton states, σ_x and σ_z are Pauli matrices acting on the two bright states

with eigenvalues of $m = \pm 1$, $\delta = \langle 3|H|3\rangle - \langle 4|H|4\rangle$, and $\kappa = \langle 3|H|4\rangle$. The bright states of the total Hamiltonian H can be constructed as a linear combination of $|3\rangle$ and $|4\rangle$:

$$\begin{pmatrix} \psi_3 \\ \psi_4 \end{pmatrix} = u(\theta) \begin{pmatrix} |3\rangle \\ |4\rangle \end{pmatrix}, \quad u(\theta) = \begin{pmatrix} \cos(\theta) & \sin(\theta) \\ -\sin(\theta) & \cos(\theta) \end{pmatrix}, \tag{4}$$

where θ is the polarization angle as shown in Fig. 1(c) and $u(\theta)$ is a SO(2) rotation matrix. Further, $\tan(\theta) = (\delta + \Delta/2)\kappa^{-1}$, where $\Delta = 2\sqrt{\delta^2 + \kappa^2}$ is the magnitude of exciton FSS. The values of κ and δ can be determined from experimental measurements of the FSS and polarization angle without an external force. In an ensemble of QDs, the V_1 potential can be treated as a random potential, and thus κ and δ can be viewed as two independent random numbers [63], for which reason QDs with a similar macroscopic structural profile (i.e., the same size and geometry) but different alloy configurations may have fairly different polarization angle and FSS.

If two bright exciton states have measurable extrinsic lifetimes $T_{3\eta}$ and $T_{4\eta}$, which are usually deduced experimentally by the fitting of the time-resolved photoluminescence spectrum to a single exponential decaying function. The difference in lifetimes gives rise to the extrinsic lifetime asymmetry δT_η:

$$\delta T_\eta = T_{3\eta} - T_{4\eta}, \quad T_{3\eta} + T_{4\eta} = 2T_\eta, \tag{5}$$

where T_η is the mean extrinsic lifetime measured from off-resonant excitation. In this measurement, we assume that the spin information in the electron-hole pairs is totally lost during the relaxation from the wetting layer to the two bright states of the exciton, and thus the two bright states are equally populated. However, those extrinsic lifetime asymmetries are not well defined for the following reasons. Firstly, the time-resolved photoluminescence spectrum is composed of two exponential decaying functions with two slightly different lifetimes [64–66], and thus $T_{3\eta}$ and $T_{4\eta}$ can be obtained only in the sense of best fitting. Secondly, the V_1 potential, which induces interstate mixing [see Eq. (4)], is not the major origin of lifetime asymmetries [43,67]. A more accurate description of lifetime asymmetries should be defined by the model of H_{2v} instead of the total Hamiltonian H.

Because lifetime asymmetries are, in general, much smaller than the mean lifetimes, we obtain

$$\frac{1}{T_{3\eta}} = \frac{\cos^2(\theta)}{\tau_{3\eta}} + \frac{\sin^2(\theta)}{\tau_{4\eta}}, \frac{1}{T_{4\eta}} = \frac{\sin^2(\theta)}{\tau_{3\eta}} + \frac{\cos^2(\theta)}{\tau_{4\eta}}. \tag{6}$$

To the leading term of $\delta\tau_\eta$, we find

$$T_{3\eta} = \tau_\eta + \frac{\cos(2\theta)}{2}\delta\tau_\eta, \quad T_{4\eta} = \tau_\eta - \frac{\cos(2\theta)}{2}\delta\tau_\eta. \tag{7}$$

The above results are identical to fitting the photoluminescence spectrum to a single exponential decaying function by minimization of the following function:

$$\mathcal{F}_n = \int_0^\infty |c_n e^{-(t/\tau_{3\eta})} + (1-c_n)e^{-(t/\tau_{4\eta})} - e^{-(t/T_\eta)}|^2 dt, \quad (8)$$

where $n = 3, 4$, with $c_3 = \cos(\theta)^2$ for $|3\rangle$ and $c_4 = \sin^2(\theta)$ for $|4\rangle$. Assuming $T_\eta = \tau_\eta + x\delta\tau_\eta$ (where $|x| \ll 1$), we obtain $\mathcal{F}_\eta = (-1 + 2c_n + 2x)^2 \delta\tau^2/16\tau + \mathcal{O}(\delta\tau/\tau)^3$. It is straightforward to obtain its solution, which is identical to ones given in Eq. (7). We therefore see that the definitions given in Eqs. (6) and (8) are equivalent in the small-asymmetry limit.

IV. THEORETICAL PREDICTIONS AND VERIFICATIONS

A. The unusual effects of low-symmetry perturbation potential

(i) Lifetime-sum rule: The weak C_1 potential will not alter the averaged exciton lifetime, which is determined as

$$T_{3\eta} + T_{4\eta} = \tau_{3\eta} + \tau_{4\eta}, \quad \tau_\eta = T_\eta. \quad (9)$$

The equality relation $\tau_\eta = T_\eta$ indicates that the mean lifetime is independent of the V_1 potential, which is manifested in the investigated QD ensembles as shown in Fig. 2.

(ii) Lifetime-asymmetry relation: The extrinsic lifetime asymmetry is determined as

$$\delta T_\eta = T_{3\eta} - T_{4\eta} = \cos(2\theta)\delta\tau_\eta \le |\delta\tau_\eta|. \quad (10)$$

We see that, to the leading term, the extrinsic lifetime asymmetries depend only on the intrinsic lifetime asymmetries $\delta\tau_\eta$ and the polarization angle θ, and are independent of the mean lifetimes τ_η and T_η. While the V_1 potential can enhance the FSS and polarization angle, it will unexpectedly suppress the magnitude of δT_η, which is upper bounded by $|\delta\tau_\eta|$. Moreover, when $\delta\tau_\eta = 0$ (in QDs with high symmetries) or $\theta = \pm(\pi/4)$ (polarized along the Γ_2 and Γ_4 directions), the change of low-symmetry potential will never induce a finite extrinsic lifetime asymmetry.

To verify the above predictions, we perform atomistic simulations for single QDs as well as QD ensembles. The calculated results for various types of single pure InAs/GaAs QDs and alloyed (In,Ga)As/GaAs QDs are summarized in Table I. For pure InAs/GaAs QDs, we find that, as expected since $V_1 = 0$, the polarization angle $\theta = 0$ (or $\pi/2$), and $\delta\tau_\eta = \delta T_\eta$, following exactly Eq. (10). The magnitude of both the intrinsic lifetime asymmetry δT_η and the extrinsic lifetime asymmetry $\delta\tau_\eta$ is in range of 0.1–0.4 ns, and is much smaller than the mean lifetimes
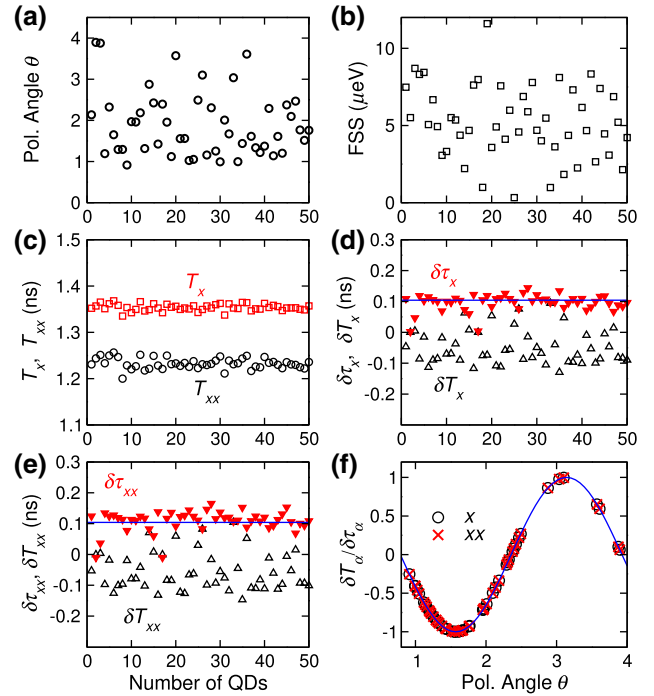

FIG. 2. Effect of random fluctuations the lifetime asymmetries in a QD ensemble. (a),(b) The calculated polarization angles and FSSs in a QD ensemble. (c) The extrinsic mean lifetimes for excitons and biexcitons [under the assumption of Eq. (9)]. (d),(e) The intrinsic and extrinsic lifetime asymmetries in a QD ensemble for excitons and biexcitiosn, where the intrinsic lifetime asymmetries are determined with the wave functions of $|3\rangle$ and $|4\rangle$ for QDs with H_{2v} symmetry. The horizontal blue lines represent the mean values of $\delta\tau_\eta$, which are 0.10 ns (approximately 9% τ_x) and 0.11 ns (approximately 10% τ_{xx}), respectively. (f) The ratio between δT_η and $\delta\tau_\eta$ will collapse to a cosine function (solid blue line) according to Eq. (10).

T_η and τ_η, which are around 1.5–2.0 ns. From Table I, we see that the lifetime-sum rule given in Eq. (9) holds for all calculated QDs, including alloyed ones. Although the polarization angles θ in alloyed QDs deviate significantly from the [110] and [1$\bar{1}$0] directions as a result of wave functions mixing, $|\delta T_\eta| \le |\delta\tau_\eta|$ holds in all QDs. Therefore, we demonstrate that the low-symmetry potential can remarkably suppress the lifetime asymmetries along with the derived relation given in Eq. (10).

We further consider the alloyed QD ensembles, in which the FSSs, polarization angles, and mean lifetimes T_η fluctuate from dot to dot over a wide range. We arbitrarily choose an alloyed (In,Ga)As/GaAs QD from Table I (No. 9) and then generate 50 different replica with randomly placed In and Ga atoms for a specific composition of 60%, which mimics an experimentally grown QD ensemble. The calculated results for this ensemble are shown in Fig. 2. As expected, the FSSs, polarization angles θ, mean lifetimes T_η, and lifetime asymmetries δT_η fluctuate from dot to dot

TABLE I. Summarized parameters for different QDs from atomistic simulation. We consider lens-shaped (L), elongated (E), and pyramidal (Py) QDs with different sizes (diameter along the [110] and [1$\bar{1}$0] directions and height along the z direction). The exciton energy, FSS, and polarization angle without an external force are shown in columns 4–6. The last eight columns present the extrinsic and intrinsic lifetime asymmetries.

No.	QD	$(d_{[110]}, d_{[1\bar{1}0]}, h)$	E_X (eV)	Δ (μeV)	θ (rad)	T_x (ns)	δT_x (ps)	τ_x (ns)	$\delta\tau_x$ (ps)	T_{xx} (ns)	δT_{xx} (ps)	τ_{xx} (ns)	$\delta\tau_{xx}$ (ps)
1	InAs(L)	25.0, 25.0, 3.0	1.01	14.7	0	1.56	134.00	1.56	134.00	1.67	144.45	1.67	144.45
2	InAs(L)	24.0, 24.0, 3.0	1.02	16.3	0	1.56	142.77	1.56	142.77	1.67	153.65	1.67	153.65
3	InAs(L)	25.0, 25.0, 4.0	0.98	8.2	0	1.84	172.55	1.84	172.55	1.96	184.84	1.96	184.84
4	InAs(L)	25.0, 20.0, 2.5	1.02	6.0	0	1.56	385.34	1.56	385.34	1.68	418.26	1.68	418.26
5	InAs(L)	25.0, 22.7, 3.0	0.99	6.1	0	1.59	244.85	1.59	244.85	1.71	265.04	1.71	265.04
6	In$_{0.6}$Ga$_{0.4}$As(L)	24.0, 24.0, 4.0	1.24	1.29	0.26	1.21	− 1.48	1.21	− 1.70	1.33	− 2.52	1.33	− 2.89
7	In$_{0.6}$Ga$_{0.4}$As(L)	25.0, 25.0, 3.0	1.25	1.35	3.05	1.29	15.52	1.29	15.81	1.40	18.1	1.40	18.45
8	In$_{0.6}$Ga$_{0.4}$As(L)	25.0, 25.0, 4.0	1.23	3.37	2.75	1.23	6.87	1.23	9.65	1.33	8.15	1.33	11.45
9	In$_{0.6}$Ga$_{0.4}$As(E)	25.0, 22.7, 3.0	1.24	7.48	2.14	1.23	− 46.45	1.23	108.85	1.35	− 52.97	1.35	124.14
10	In$_{0.6}$Ga$_{0.4}$As(E)	25.0, 30.0, 4.5	1.21	4.23	1.91	1.13	− 147.54	1.13	188.57	1.26	− 166.49	1.26	212.80
11	In$_{0.6}$Ga$_{0.4}$As(Py)	25.0, 25.0, 3.0	1.28	7.18	2.85	1.43	− 3.0	1.43	− 3.59	1.53	− 2.91	1.53	− 3.49
12	In$_{0.6}$Ga$_{0.4}$As(Py)	25.0, 25.0, 4.0	1.25	6.44	2.86	1.30	− 8.64	1.30	− 10.19	1.41	− 11.62	1.41	− 13.70

over a wide range within an ensemble. Because all modeled dots within the ensemble have the same shape, size, and alloy composition, they almost share the same H_{2v} Hamiltonian, which means their intrinsic properties should be similar. Indeed, the deduced intrinsic lifetime asymmetries $\delta\tau_\eta$ are rather insensitive to alloy-atom fluctuations in an ensemble. The observed fluctuations in the extrinsic quantities of FSSs, θ, T_η, and δT_η, are attributed to alloy-fluctuation-induced change of the V_1 potential. We find that $|\delta T_\eta| \leq |\delta\tau_\eta|$ for all dots [see Figs. 2(d) and 2(e)], and the ratios of the extrinsic and intrinsic lifetime asymmetries fall on a cosine curve as shown in Fig. 2(f), consistent with the prediction given in Eq. (10). The alloy-induced V_1 perturbation potential remarkably reduces extrinsic lifetime asymmetries δT_η to around zero, in contrast to their intrinsic lifetime asymmetry of around 0.1 ns.

B. The optical anisotropy relying on the intrinsic lifetimes

The signals collected along the ϕ direction after off-resonance excitation can be written as

$$I_\eta(\phi) \propto 1 + \cos(2\theta)\cos[2(\phi-\theta)]\frac{\delta\tau_\eta}{2\tau_\eta}, \quad (11)$$

where ϕ is the angle relative to the [110] direction. Here we also assume that both bright states are equally occupied from off-resonance excitation in the same way as we developed Eq. (9). We obtain the maximum degree of linear polarization $\rho_{\eta,\text{max}}$ when $\phi = \theta$ or $\theta + \pi/2$:

$$\rho_{\eta,\text{max}} = \frac{I_\text{max} - I_\text{min}}{I_\text{max} + I_\text{min}} = \left|\frac{\cos(2\theta)\delta\tau_\eta}{2\tau_\eta}\right| \leq \left|\frac{\delta\tau_\eta}{2\tau_\eta}\right|. \quad (12)$$

The degree of polarization is determined fully by the polarizaton angle θ, lifetime asymmetry $\delta\tau_\eta$, and mean

lifetime τ_η, considering that the transition between two bright exciton states is strictly forbidden by the selection rule. The degree of polarization is upper bounded by $|\delta\tau_\eta/\tau_\eta|/2$. Regarding $|\delta\tau_\eta| \ll \tau_\eta$, the degree of polarization is restricted to a small magnitude despite the large variation from dot to dot. The polarization discussed here should be different from the linear polarization defined in some experiments, in which the excitation and measurement are performed along two orthogonal directions, and thus the degree of polarizations are generally in the order of 80%–90% of the available experimental data [68–71]. In the latter case, polarization is complicated since carrier scattering, spin flipping, and lifetime asymmetry all contribute to its nonunity.

For the measurement along the [110] and [1$\bar{1}$0] directions (let $\phi = 0$),

$$\rho_{\eta,\times} = \frac{I_{[110]} - I_{[1\bar{1}0]}}{I_{[110]} + I_{[1\bar{1}0]}} = \frac{\cos^2(2\theta)\delta\tau_\eta}{2\tau_\eta}, \quad (13)$$

which is smaller than $\rho_{\eta,\text{max}}$ by a factor of $\cos(2\theta)$. We further prove straightforwardly that the degree of linear polarization along the x and y directions is $\rho_{\eta,+} = \sin(2\theta)\rho_{\eta,\text{max}}$. The relations between these degrees of polarization are presented in Fig. 3. Although the small extrinsic lifetime asymmetry may be hard to measure directly by fitting the time-dependent photoluminescence with two exponential decaying functions, the relative polarization angle θ, the mean lifetime τ_η [see Eq. (9)], and the degree of polarization $\rho_{\eta,i}$ can be measured precisely, thus making it rather feasible to obtain the intrinsic lifetime asymmetries $\delta\tau_\eta$ in experiments. Once we obtain the intrinsic lifetime asymmetry $\delta\tau_\eta$, the extrinsic lifetime asymmetry δT_η can be deduced with use of Eq. (10).
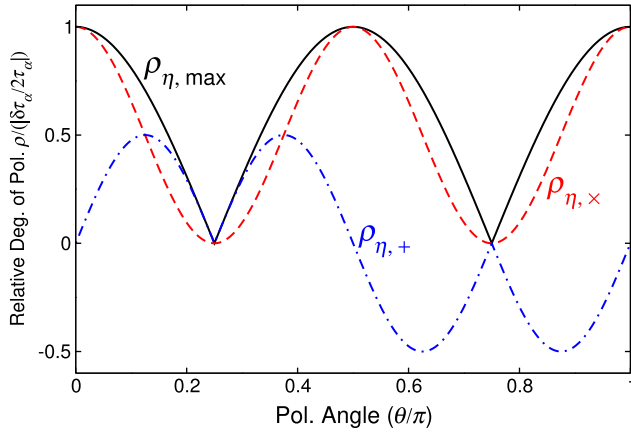
FIG. 3.   Relative relations between different degrees of polarization as a function of polarization angle for an alloyed QD.

C. The optical polarization relying on the intrinsic lifetimes

Since exciton and biexciton states possess the same polarization angle θ, we obtain

$$\frac{\rho_{x,i}}{\rho_{xx,i}} = \frac{\delta\tau_x}{\delta\tau_{xx}} \cdot \frac{\tau_{xx}}{\tau_x}, \quad i = \{\max, \times, +\}, \qquad (14)$$

which is also independent of the measured ϕ. The deduced relations for the degree of polarization with intrinsic lifetimes τ_η and lifetime asymmetry $\delta\tau_\eta$ of the H_{2v} term along various directions can be examined with the data from atomistic calculations shown in Fig. 2. For this QD ensemble, $\delta\tau_\eta \sim 0.1$ ns and $\tau_\eta \sim 1.25$–1.35 ns, and thus $\rho_{\eta,\max} \lesssim \delta\tau_\eta/2\tau_\eta \sim 4\%$, which is in good agreement with the atomistic-simulation-predicted upper bound of the degree of polarization of approximately 4% as shown in Fig. 2(a). We may also calculate the ratio of the degree of polarization for excitons and biexcitons, which is independent of the direction of the optical measurements. This ratio is $\rho_{x,i}/\rho_{xx,i} \sim 1.08$. We expect this ratio to become larger for QDs with large shape asymmetry (such as elongation). In principle, the evolution of linear polarization as a function of angle ϕ [Eq. (11)] can be obtained by careful calibration of the light path in experiments.

D. The quadratic and strong nonlinear responses of the extrinsic lifetimes to external stress

In the presence of weak external force F, the effective Hamiltonian becomes [45–48]

$$H = E_0 + (\alpha F + \delta)\sigma_z + (\kappa + \beta F)\sigma_x, \qquad (15)$$

where the extra perturbative term $\delta V = V_s F$ is responsible for the applied external force. The symmetry of δV depends strongly on the directions and the ways in which the forces are applied (see Fig. 4). Here, we consider only the case

with a single external force, and generalization of this theory to multiple forces is straightforward following Refs. [46–48] due to additivity of the C_1 potentials. Notice that two unperturbed (intrinsic) bright exciton states $|3\rangle$ and $|4\rangle$ are also functions of F because H_{2v} should also be force dependent. For the stress applied along the [110] direction, the strained Hamiltonian still keeps C_{2v} symmetry [see Figs. 4(a) and 4(c)], and thus stress-induced coupling between the two bright states is forbidden. This is different from the case along the [100] direction, where the stress induces not only coupling of bright exciton states to highly excited states arising from other bands (termed "interband coupling") but also coupling between two bright exciton states (termed "intraband coupling") [see Figs. 4(b) and 4(d)]. The linear coupling dominates the interband coupling due to the large energy separation (approximately 40–100 meV) between the ground s band and the excited p and d bands, while the nonlinear effect may become significant in intraband coupling due to the much smaller energy difference between these two bright exciton states. This difference has remarkable consequences for the lifetime asymmetries. According to perturbation theory, we rewrite the intrinsic lifetimes as

$$\frac{1}{\tau_i^\eta(F)} = \frac{1}{\tau_i^\eta} + \gamma_i^\eta F + \xi_i^\eta F^2, \qquad (16)$$
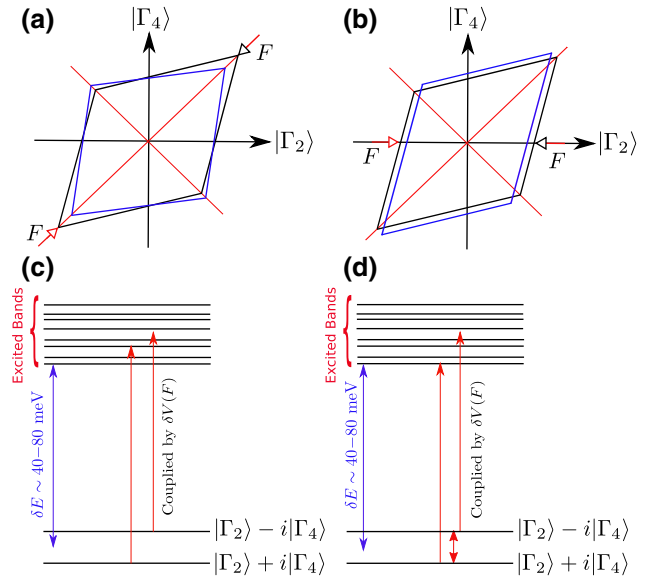

FIG. 4.   Effect of external stress on QDs. (a),(b) The role of stress along the [110] and [100] directions, respectively. The black and blue boxes represent the QDs before and after being stressed. (c),(d) The coupling between the bright states and the excited states caused by stress along different directions. In these two cases the strain Hamiltonian may have different symmetries, and thus the coupling between the bright states and the excited states and the direction coupling among the two bright states are totally different.

for $i = 3, 4$ and $\eta = \{x, xx\}$. Here we have introduced two new parameters γ_i^η and ξ_i^η to characterize the linear and quadratic dependence on external force, respectively. When the contributions of the second and third terms are small as compared with $1/\tau_i^\eta$, we obtain

$$\tau_i^\eta(F) = \tau_i^\eta - (\tau_i^\eta)^2[\gamma_i^\eta F + \xi_i^\eta F^2 - (\gamma_i^\eta)^2\tau_i^\eta F^2], \quad (17)$$

which is again a quadratic function of F. It it expected that $\tau_\eta = (\tau_3^\eta + \tau_4^\eta)/2$ and $\delta\tau_\eta = (\tau_3^\eta - \tau_4^\eta)/2$ are also linear and/or quadratic functions of F. With these defined intrinsic lifetime asymmetries, the extrinsic lifetimes and their asymmetries can be obtained via

$$\delta T_\eta(F) = \cos[2\theta(F)]\delta\tau_\eta(F), \quad T_\eta(F) = \tau_\eta(F). \quad (18)$$

The striking consequence is that even under a weak force the extrinsic lifetime asymmetry δT_η is not necessarily a simple quadratic function of F due to the presence of the strong nonlinear cosine term. We can derive more exact relations via a combination of the current results and results in previous literature [45,47,48].

We next attempt to study the evolution of optical properties of QDs under external forces, which enables us to verify the last and the most intriguing prediction [Eq. (18)] in this work. The properties of QDs fluctuate strongly from

dot to dot; therefore investigation in single QDs could provide more convincing evidence for our predictions. We consider the pure InAs/GaAs QD (No. 3 in Table I) and alloyed (In,Ga)As/GaAs QD (No. 12 in Table I) under uniaxial stress along the [110] and [100] directions, respectively. Figure 5 shows calculated FSSs and polarization angles as functions of stress for these two QDs obtained with the atomistic method, accompanied by fitted results obtained with the two-level model. We demonstrate that we can tune the FSS to zero on applying a stress along the [110] direction, which does not lower the QD symmetry [see Fig. 4], for the pure QDs, but it is impossible for alloyed QDs, where the achievable minimum lower bound of FSS is significantly larger than the spontaneous broadening of the spectra Γ [8–10]. This large minimum FSS implies that we cannot eliminate the FSS of alloyed QDs by using a single external force.

Figure 6 shows calculated intrinsic lifetimes and their asymmetries as functions of applied stress for both pure InAs/GaAs and alloyed (In,Ga)As/GaAs QDs. For stress applied along the [110] direction, we find that τ_{3x} and
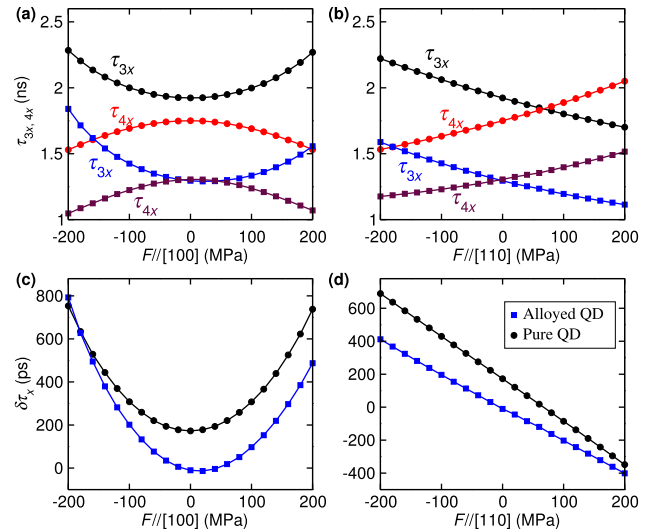
FIG. 6. Linear and quadratic relations for intrinsic lifetime asymmetries. The solid squares represent the pure QDs, while the solid circles represent the alloyed QDs along (a),(c) the [100] direction and (b),(d) the [110] direction obtained from the atomistic simulation. The solid lines are fitted with a quadratic function of F, and for the solid lines the parameters (in the unit of nanoseconds per megapascal for ξ_i^x and nanoseconds per megapascal squared for γ_i^x) used are as follows: for pure QDs along the [100] direction, $\gamma_3^x = 6.73 \times 10^{-6}$, $\xi_3^x = -2.29 \times 10^{-6}$, $\gamma_4^x = 7.53 \times 10^{-7}$, and $\xi_4^x = 1.83 \times 10^{-6}$; for pure QDs along the [110] direction, $\gamma_3^x = 3.52 \times 10^{-4}$, $\xi_3^x = -2.31 \times 10^{-8}$, $\gamma_4^x = -4.20 \times 10^{-4}$, and $\xi_4^x = -2.30 \times 10^{-8}$; for alloyed QDs along the [100] direction, $\gamma_3^x = 3.45 \times 10^{-4}$, $\xi_3^x = -5.53 \times 10^{-6}$, and $\gamma_4^x = -3.51 \times 10^{-5}$, $\xi_4^x = 3.82 \times 10^{-6}$; for alloyed QDs along the [110] direction, $\gamma_3^x = 7.00 \times 10^{-4}$, $\xi_3^x = -2.18 \times 10^{-7}$, $\gamma_4^x = -4.95 \times 10^{-4}$, and $\xi_4^x = -2.58 \times 10^{-7}$.
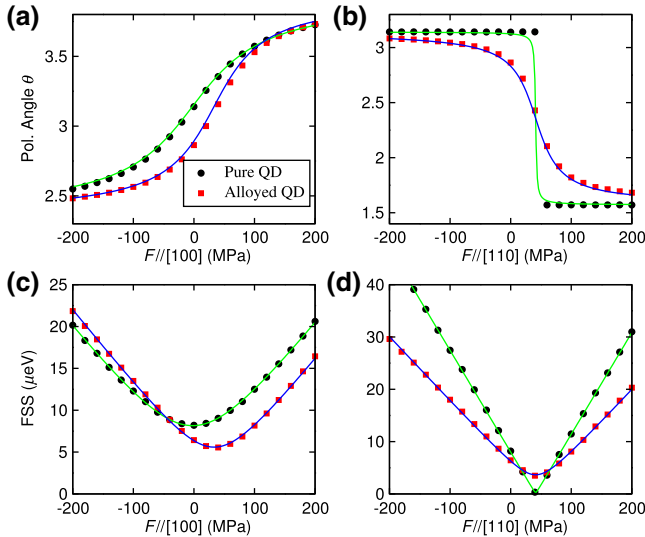

FIG. 5. Polarization angle and FSS in pure and alloyed QDs under stress. (a),(c) The results for stress along the [100] direction. (b),(d) The results for stress along the [110] direction. The open symbols represent the data from the atomistic simulation, while the solid line is the fitting obtained with the effective two-band model with the following parameters in the unit of microelectronvolts for δ and κ and microelectronvolts per megapascal for α and β: for pure QDs, $\delta = 2.73$, $\kappa = -1.69$, $\alpha_{[100]} = 0$, $\beta_{[100]} = 0.05$, and $\alpha_{[110]} = -0.12$, $\beta_{[110]} = 0$; for alloyed QDs, $\delta = 4.1$, $\kappa = -0.02$, $\alpha_{[100]} = 0$, $\beta_{[100]} = 0.05$, and $\alpha_{[110]} = -0.19$, $\beta_{[110]} = 0$.
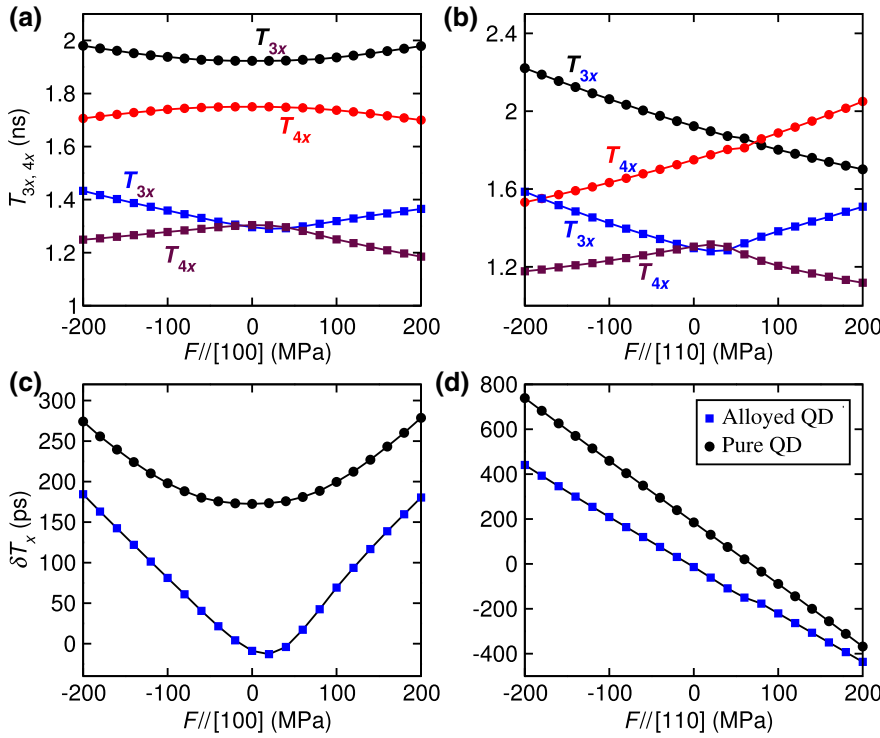
FIG. 7. Strong nonlinearity in extrinsic lifetimes and extrinsic lifetime asymmetries. The solid squares and solid circles show the results for alloyed and pure QDs, respectively. The solid line is computed with parameters from Fig. 6 and with use of Eq. (18).

τ_{4x} are linear functions of stress F, as shown in Figs. 6(b)–6(d). To further verify their linear feature, we fit these data to quadratic functions. We gain tiny coefficients of the quadratic terms for both pure InAs/GaAs and alloyed (In,Ga)As/GaAs QDs ($\xi_{3,4}^x \sim 10^{-8}$–10^{-7} ns/MPa^2; see fitted data in Fig. 6), which illustrates that both intrinsic lifetimes and their asymmetries are linear versus stress along the [110] direction. In striking contrast to the [110] direction, stress applied along the [100] direction gives rise to a different response of the lifetime of τ_{3x} and τ_{4x}, because it causes direct coupling between two bright exciton states (see the mechanism in Fig. 4). From Fig. 6, we see that both τ_{3x} and τ_{4x} exhibit quadratic relations with regard to applied stress F along the [100] direction. As expected, the corresponding lifetime asymmetry $\delta\tau_x$ is also a quadratic function of F. Similar features can also be found for transition from biexciton to exciton states.

The extrinsic lifetime asymmetries have more complicated response behaviors to applied stress and will exhibit strong nonlinearity even under a weak force due to direct coupling between the two bright states induced by the C_1 symmetry potential V_1. Figure 7 shows atomistic calculated results. In the pure InAs/GaAs QD, the V_1 potential is absent, and thus T_{3x} and T_{4x} should be perfect linear functions of F for stress applied along the [110] direction and quadratic functions for stress applied along the [100] direction. The results shown in Fig. 7 well support the theoretical prediction. These stress responses are identical to τ_η, as shown in Figs. 6(b) and 6(d), in the sense that $\theta = 0$. However, for alloyed (In,Ga)As/GaAs QDs,

strong nonlinearity behaviors of both the mean extrinsic lifetimes and extrinsic lifetime asymmetries are expected for stress applied along the [100] and [110] directions. Since $T_i(F) = \tau_i(F)$ [see Eq. (18)], we observe the strong nonlinearity in both the extrinsic lifetimes $T_{i\eta}$ and the extrinsic lifetime asymmetries δT_η. Moreover, while the extrinsic lifetime asymmetries are generally very small due to a wave-function-mixing effect, we find that the extrinsic lifetime asymmetries in Figs. 7(c) and 7(d) and the intrinsic lifetime asymmetries in Figs. 6(c) and 6(d) can be pronouncedly enhanced by external stress from tens of picoseconds to 0.2–0.7 ns (i.e., by at least 1 order of magnitude). These enhanced asymmetries may lead to direct measurement of lifetime asymmetries with only the time-resolved photoluminescnce spectrum, which should be fitted with two exponential decaying functions. A similar strong nonlinearity effect is also observed for transition from biexciton to exciton states for the reason discussed above. These results can be well described by the data in Fig. 6 and are in full accordance with our theoretical predictions.

V. SUMMARY

We introduce lifetime asymmetry into self-assembled QDs. We reveal that intrinsic lifetimes are fundamental quantities of QDs, which determine the bound of the extrinsic lifetime asymmetries, polarization angles, FSSs, and their evolution under uniaxial external forces. These predictions can be measured directly or extracted from

experiments using the state-of-the-art techniques, such as the measured linear polarization as well as the optical properties of QDs under external forces. We verify these predictions using atomistic simulations. We find that the intrinsic lifetime asymmetries can be on the order of few hundred picoseconds in pure InAs/GaAs QDs, but the extrinsic lifetime asymmetries can be much smaller in alloyed (In,Ga)As/GaAs QDs. However, the lifetime asymmetries are susceptible to external forces and their directions, and thus can be more conclusively verified by investigation of their behaviors under external forces. These relations represent a complete description of the optical properties of QDs. Our findings can provide an important basis to deepen our understanding of QDs.

---

[1] O. Benson, C. Santori, M. Pelton, and Y. Yamamoto, Regulated and Entangled Photons from a Single Quantum Dot, Phys. Rev. Lett. **84**, 2513 (2000).

[2] J. W. Pan, D. Bouwmeester, H. Weinfurter, and A. Zeilinger, Experimental Entanglement Swapping: Entangling Photons that Never Interacted, Phys. Rev. Lett. **80**, 3891 (1998).

[3] N. Gisin, G. Ribordy, W. Tittel, and H. Zbinden, Quantum cryptography, Rev. Mod. Phys. **74**, 145 (2002).

[4] L. M. Duan, M. D. Lukin, J. I. Cirac, and P. Zoller, Long-distance quantum communication with atomic ensembles and linear optics, Nature **414**, 413 (2001).

[5] J. S. Xu, C. F. Li, M. Gong, X. B. Zou, C. H. Shi, G. Chen, and G. C. Guo, Experimental Demonstration of Photonic Entanglement Collapse and Revival, Phys. Rev. Lett. **104**, 100502 (2010).

[6] Y. F. Huang, B. H. Liu, L. Peng, Y. H. Li, L. Li, C. F. Li, and G. C. Guo, Experimental generation of an eight-photon Greenberger-Horne-Zeilinger state, Nat. Commun. **2**, 546 (2011).

[7] J. Yin, Y. Cao, Y. H. Li, S. K. Liao, L. Zhang, J. G. Ren, W. Q. Cai, and W. Y. Liu *et al.*, Satellite-based entanglement distribution over 1200 kilometers, Science **356**, 1140 (2017).

[8] D. Gammon, E. S. Snow, B. V. Shanabrook, D. S. Katzer, and D. Park, Fine Structure Splitting in the Optical Spectra of Single GaAs Quantum Dots, Phys. Rev. Lett. **76**, 3005 (1996).

[9] M. Bayer, G. Ortner, O. Stern, A. Kuther, A. A. Gorbunov, A. Forchel, P. Hawrylak, S. Fafard, K. Hinzer, T. L. Reinecke, S. N. Walck, J. P. Reithmaier, F. Klopf, and F. Schafer, Fine structure of neutral and charged excitons in self-assembled In(Ga)As/(Al)GaAs quantum dots, Phys. Rev. B **65**, 195315 (2002).

[10] R. Seguin, A. Schliwa, S. Rodt, K. Potschke, U. W. Pohl, and D. Bimberg, Size-dependent Fine-structure Splitting in Self-organized InAs/GaAs Quantum Dots, Phys. Rev. Lett. **95**, 257402 (2005).

[11] W. Langbein, P. Borri, U. Woggon, V. Stavarache, D. Reuter, and A. D. Wieck, Control of fine-structure splitting and biexciton binding in In$_x$Ga$_{1-x}$As quantum dots by annealing, Phys. Rev. B **69**, 161301(R) (2004).

[12] A. I. Tartakovskii, M. N. Makhonin, I. R. Sellers, J. Cahill, A. D. Andreev, D. M. Whittaker, J. P. R. Wells, A. M. Fox, D. J. Mowbray, M. S. Skolnick, K. M. Groom, M. J. Steer, H. Y. Liu, and M. Hopkinson, Effect of thermal annealing and strain engineering on the fine structure of quantum dot excitons, Phys. Rev. B **70**, 193303 (2004).

[13] D. J. P. Ellis, R. M. Stevenson, R. J. Young, A. J. Shields, P. Atkinson, and D. A. Ritchie, Control of fine-structure splitting of individual InAs quantum dots by rapid thermal annealing, Appl. Phys. Lett. **90**, 011907 (2007).

[14] R. Seguin, A. Schliwa, T. D. Germann, S. Rodt, K. Pötschke, A. Strittmatter, U. W. Pohl, D. Bimberg, M. Winkelnkemper, T. Hammerschmidt, and P. Kratzer, Control of fine-structure splitting and excitonic binding energies in selected individual InAs/GaAs quantum dots, Appl. Phys. Lett. **89**, 263109 (2006).

[15] A. I. Tartakovskii, M. N. Makhonin, I. R. Sellers, J. Cahill, A. D. Andreev, D. M. Whittaker, J. P. R. Wells, A. M. Fox, D. J. Mowbray, M. S. Skolnick, K. M. Groom, M. J. Steer, H. Y. Liu, and M. Hopkinson, Effect of thermal annealing and strain engineering on the fine structure of quantum dot excitons, Phys. Rev. B **70**, 193303 (2004).

[16] B. D. Gerardot, S. Seidl, P. A. Dalgarno, R. J. Warburton, D. Granados, J. M. Garcia, K. Kowalik, O. Krebs, K. Karrai, A. Badolato, and P. M. Petroff, Manipulating exciton fine structure in quantum dots with a lateral electric field, Appl. Phys. Lett. **90**, 041101 (2007).

[17] K. Kowalik, O. Krebs, A. Lematre, S. Laurent, P. Senellart, P. Voisin, and J. A. Gaj, Influence of an in-plane electric field on exciton fine structure in InAs-GaAs self-assembled quantum dots, Appl. Phys. Lett. **86**, 041907 (2005).

[18] M. M. Vogel, S. M. Ulrich, R. Hafenbrak, P. Michler, L. Wang, A. Rastelli, and O. G. Schmidt, Influence of lateral electric fields on multiexcitonic transitions and fine structure of single quantum dots, Appl. Phys. Lett. **91**, 051904 (2007).

[19] M. Ghali, K. Ohtani, Y. Ohno, and H. Ohno, Generation and control of polarization-entangled photons from GaAs island quantum dots by an electric field, Nat. Commun. **3**, 661 (2012).

[20] A. J. Bennett, M. A. Pooley, R. M. Stevenson, M. B. Ward, R. B. Patel, A. Boyer de la Giroday, N. Sköld, I. Farrer, C. A. Nicoll, D. A. Ritchie, and A. J. Shields, Electric-field-induced coherent coupling of the exciton states in a single quantum dot, Nat. Phys. **6**, 947 (2010).

[21] J. Tang, S. Cao, Y. Gao, Y. Sun, W. Geng, D. A. Williams, K. Jin, and X. Xu, Charge state control in single InAs/GaAs quantum dots by external electric and magnetic fields, Appl. Phys. Lett. **105**, 041109 (2014).

[22] J. D. Mar, J. J. Baumberg, X. L. Xu, A. C. Irvine, and D. A. Williams, Electrical control of quantum-dot fine-structure splitting for high-fidelity hole spin initialization, Phys. Rev. B **93**, 045316 (2016).

[23] J. D. Mar, X. L. Xu, J. S. Sandhu, A. C. Irvine, M. Hopkinson, and D. A. Williams, Electrical control of fine-structure splitting in self-assembled quantum dots for entangled photon pair creation, Appl. Phys. Lett. **97**, 221108 (2010).

[24] P. Mrowiński, A. Musiał, A. Maryński, M. Syperek, J. Misiewicz, A. Somers, J. P. Reithmaier, S. Höfling, and G. Sęk, Magnetic field control of the neutral and charged exciton fine structure in single quantum dashes emitting at 1.55 μm, Appl. Phys. Lett. **106**, 053114 (2015).

[25] R. M. Stevenson, R. J. Young, P. See, D. G. Gevaux, K. Cooper, P. Atkinson, I. Farrer, D. A. Ritchie, and A. J. Shields, Magnetic-field-induced reduction of the exciton polarization splitting in InAs quantum dots, Phys. Rev. B **73**, 033306 (2006).

[26] J. Puls, M. Rabe, H. J. Wunsche, and F. Henneberger, Magneto-optical study of the exciton fine structure in self-assembled CdSe quantum dots, Phys. Rev. B **60**, R16303(R) (1999).

[27] R. M. Stevenson, R. J. Young, P. Atkinson, K. Cooper, D. A. Ritchie, and A. J. Shields, A semiconductor source of triggered entangled photon pairs, Nature **439**, 179 (2006).

[28] C. E. Kuklewicz, R. N. E. Malein, P. M. Petroff, and B. D. Gerardot, Electro-elastic tuning of single particles in individual self-assembled quantum dots, Nano Lett. **12**, 3761 (2012).

[29] F. Ding, R. Singh, J. D. Plumhof, T. Zander, V. Křápek, Y. H. Chen, M. Benyoucef, V. Zwiller, K. Dörr, G. Bester, A. Rastelli, and O. G. Schmidt, Tuning the Exciton Binding Energies in Single Self-assembled InGaAs/GaAs Quantum Dots by Piezoelectric-induced Biaxial Stress, Phys. Rev. Lett. **104**, 067405 (2010).

[30] J. D. Plumhof, V. Křápek, F. Ding, K. D. Jöns, R. Hafenbrak, P. Klenovský, A. Herklotz, K. Dörr, P. Michler, A. Rastelli, and O. G. Schmidt, Strain-induced anticrossing of bright exciton levels in single self-assembled GaAs/Al$_x$Ga$_{1-x}$As and In$_x$Ga$_{1-x}$As/GaAs quantum dots, Phys. Rev. B **83**, 121302(R) (2011).

[31] A. Rastelli, F. Ding, J. D. Plumhof, S. Kumar, R. Trotta, Ch. Deneke, A. Malachias, P. Atkinson, E. Zallo, T. Zander, A. Herklotz, R. Singh, V. Křápek, J. R. Schröter, S. Kiravittaya, M. Benyoucef, R. Hafenbrak, K. D. Jöns, D. J. Thurmer, D. Grimm, G. Bester, K. Dörr, P. Michler, and O. G. Schmidt, Controlling quantum dot emission by integration of semiconductor nanomembranes onto piezoelectric actuators, Phys. Status Solidi B **249**, 687 (2012).

[32] R. Trotta, P. Atkinson, J. D. Plumhof, E. Zallo, R. O. Rezaev, S. Kumar, S. Baunack, R. Schröter, J. A. Rastelli, and O. G. Schmidt, Nanomembrane quantum-light-emitting diodes integrated onto piezoelectric actuators, Adv. Mater. **24**, 2668 (2012).

[33] R. Trotta, E. Zallo, C. Ortix, P. Atkinson, J. D. Plumhof, J. van den Brink, A. Rastelli, and O. G. Schmidt, Universal Recovery of the Energy-level Degeneracy of Bright Excitons in InGaAs Quantum Dots Without a Structure Symmetry, Phys. Rev. Lett. **109**, 147401 (2012).

[34] J. D. Plumhof, R. Trotta, V. Křápek, E. Zallo, P. Atkinson, S. Kumar, A. Rastelli, and O. G. Schmidt, Tuning of the valence band mixing of excitons confined in GaAs/AlGaAs quantum dots via piezoelectric-induced anisotropic strain, Phys. Rev. B **87**, 075311 (2013).

[35] S. Kumar, E. Zallo, Y. H. Liao, P. Y. Lin, R. Trotta, P. Atkinson, J. D. Plumhof, F. Ding, B. D. Gerardot, S. J. Cheng, A. Rastelli, and O. G. Schmidt, Anomalous anticrossing of neutral exciton states in GaAs/AlGaAs quantum dots, Phys. Rev. B **89**, 115309 (2014).

[36] R. Trotta, J. S. Wildmann, E. Zallo, O. G. Schmidt, and A. Rastelli, Highly entangled photons from hybrid piezoelectric-semiconductor quantum dot devices, Nano Lett. **14**, 3439 (2014).

[37] R. Trotta, J. Martín-Sánchez, J. S. Wildmann, G. Piredda, M. Reindl, C. Schimpf, E. Zallo, S. Stroj, J. Edlinger, and A. Rastelli, Wavelength-tunable sources of entangled photons interfaced with atomic vapours, Nat. Commun. **7**, 10375 (2015).

[38] B. Höfer, J. Zhang, J. Wildmann, E. Zallo, R. Trotta, A. Rastelli, and O. G. Schmidt, Independent tuning of excitonic emission energy and decay time in single semiconductor quantum dots, Appl. Phys. Lett. **110**, 151102 (2017).

[39] R. Hafenbrak, S. M. Ulrich, P. Michler, L. Wang, A. Rastelli, and O. G. Schmidt, Triggered polarization-entangled photon pairs from a single quantum dot up to 30 K, New J. Phys. **9**, 315 (2007).

[40] G. Bester, S. Nair, and A. Zunger, Pseudopotential calculation of the excitonic fine structure of million-atom self-assembled In$_{1-x}$Ga$_x$As/GaAs quantum dots, Phys. Rev. B **67**, 161306(R) (2003).

[41] G. Bester and A. Zunger, Cylindrically shaped zinc-blende semiconductor quantum dots do not have cylindrical symmetry: Atomistic symmetry, atomic relaxation, and piezoelectric effects, Phys. Rev. B **71**, 045318 (2005).

[42] J. W. Luo, G. Bester, and A. Zunger, Supercoupling between heavy-hole and light-hole states in nanostructures, Phys. Rev. B **92**, 165301 (2015).

[43] R. Singh and G. Bester, Nanowire Quantum Dots as an Ideal Source of Entangled Photon Pairs, Phys. Rev. Lett. **103**, 063601 (2009).

[44] R. Singh and G. Bester, Lower Bound for the Excitonic Fine Structure Splitting in Self-assembled Quantum Dots, Phys. Rev. Lett. **104**, 196803 (2010).

[45] M. Gong, W. Zhang, G. C. Guo, and L. He, Exciton Polarization, Fine-structure Splitting, and the Asymmetry of Quantum Dots under Uniaxial Stress, Phys. Rev. Lett. **106**, 227401 (2011).

[46] L. Sapienza, R. N. E. Malein, C. E. Kuklewicz, P. E. Kremer, K. Srinivasan, A. Griffiths, E. Clarke, M. Gong, R. J. Warburton, and B. D. Gerardot, Exciton fine-structure splitting of telecom-wavelength single quantum

dots: Statistics and external strain tuning, Phys. Rev. B **88,** 155330 (2013).

[47] J. Wang, M. Gong, G. C. Guo, and L. He, Eliminating the fine structure splitting of excitons in self-assembled InAs/GaAs quantum dots via combined stresses, Appl. Phys. Lett. **101,** 063114 (2012).

[48] J. Wang, M. Gong, G. C. Guo, and L. He, Towards Scalable Entangled Photon Sources with Self-assembled InAs/GaAs Quantum Dots, Phys. Rev. Lett. **115,** 067401 (2015).

[49] R. Trotta, J. Martín-Sánchez, I. Daruka, C. Ortix, and A. Rastelli, Energy-tunable Sources of Entangled Photons: A Viable Concept for Solid-State-Based Quantum Relays, Phys. Rev. Lett. **114,** 150502 (2015).

[50] J. Zhang, J. S. Wildmann, F. Ding, R. Trotta, Y. Huo, E. Zallo, D. Huber, A. Rastelli, and O. G. Schmidt, High yield and ultrafast sources of electrically triggered entangled-photon pairs based on strain-tunable quantum dots, Nat. Commun. **6,** 10067 (2015).

[51] Y. Chen, J. Zhang, M. Zopf, K. Jung, Y. Zhang, R. Keil, F. Ding, and O. G. Schmidt, Wavelength-tunable entangled photons from silicon-integrated III-V quantum dots, Nat. Commun. **7,** 10387 (2016).

[52] R. Keil, M. Zopf, Y. Chen, B. Hoefer, J. Zhang, F. Ding, and O. G. Schmidt, Solid-state ensemble of highly entangled photon sources at rubidium atomic transitions, Nat. Commun. **8,** 15501 (2016).

[53] J. Zhang, F. Ding, E. Zallo, R. Trotta, B. Höfer, L. Han, S. Kumar, Y Huo, A. Rastelli, and O. G. Schmidt, A nanomembrane-based wavelength-tunable high-speed single-photon-emitting diode, Nano Lett. **13,** 5808 (2013).

[54] H. Huang, R. Trotta, Y. Huo, T. Lettner, J. S. Wildmann, J. Martín-Sánchez, D. Huber, M. Reindl, J. Zhang, E. Zallo, O. G. Schmidt, and A. Rastelli, Electrically-pumped wavelength-tunable GaAs quantum dots interfaced with rubidium atoms, ACS Photonics **4,** 868 (2017).

[55] G. F. Koster, J. O. Dimmock, R. G. Wheeler, and H. Statz, *Properties of the Thirty-Two Point Groups* (MIT Press, Cambridge, MA, 1963).

[56] L. W. Wang and A. Zunger, Linear combination of bulk bands method for large-scale electronic structure calculations on strained nanostructures, Phys. Rev. B **59,** 15806 (1999).

[57] A. J. Williamson, L. W. Wang, and A. Zunger, Theoretical interpretation of the experimental electronic structure of lens-shaped self-assembled InAs/GaAs quantum dots, Phys. Rev. B **62,** 12963 (2000).

[58] P. N. Keating, Effect of invariance requirements on the elastic strain energy of crystals with application to the diamond structure, Phys. Rev. **145,** 637 (1966).

[59] R. M. Martin, Elastic properties of ZnS structure semiconductors, Phys. Rev. B **1,** 4005 (1970).

[60] A. Franceschetti, H. Fu, L. W. Wang, and A. Zunger, Many-body pseudopotential theory of excitons in InP and CdSe quantum dots, Phys. Rev. B **60,** 1819 (1999).

[61] J. J. Sakurai, in, *Modern Quantum Mechanics*, edited by San Fu Tuan (Benjamin/Cummings, Menlo Park, CA, 1985), p. 276.

[62] M. Bayer, O. Stern, A. Kuther, and A. Forchel, Spectroscopic study of dark excitons in $In_xGa_{1-x}As$ self-assembled quantum dots by a magnetic-field-induced symmetry breaking, Phys. Rev. B **61,** 7273 (2000).

[63] M. Gong, B. Hofer, E. Zallo, R. Trotta, J. W. Luo, O. G. Schmidt, and C. Zhang, Statistical properties of exciton fine structure splitting and polarization angles in quantum dot ensembles, Phys. Rev. B **89,** 205312 (2014).

[64] K. Mukai, N. Ohtsuka, H. Shoji, and M. Sugawara, Phonon bottleneck in self-formed $In_xGa_{1-x}As$/GaAs quantum dots by electroluminescence and time-resolved photoluminescence, Phys. Rev. B **54,** R5243 (1996).

[65] T. Inokuma, T. Arai, and M. Ishikawa, Size effects on the temporal dynamics of edge emission in CdSe microcrystals embedded in a germanate glass matrix, Phys. Rev. B **42,** 11093 (1990).

[66] W. G. J. H. M. van Sark, P. L. T. M. Frederix, A. A. Bol, H. C. Gerritsen, and A. Meijerink, Blueing, bleaching, and blinking of single CdSe/ZnS quantum dots, Chem. Phys. Chem. **3,** 871 (2002).

[67] M. A. Dupertuis, K. F. Karlsson, D. Y. Oberli, E. Pelucchi, A. Rudra, P. O. Holtz, and E. Kapon, Symmetries and the Polarized Optical Spectra of Exciton Complexes in Quantum Dots, Phys. Rev. Lett. **107,** 127403 (2011).

[68] V. D. Kulakovskii, G. Bacher, R. Weigand, T. Kümmell, A. Forchel, E. Borovitskaya, K. Leonardi, and D. Hommel, Fine Structure of Biexciton Emission in Symmetric and Asymmetric CdSe/ZnSe Single Quantum Dots, Phys. Rev. Lett. **82,** 1780 (1999).

[69] S. M. Ulrich, S. Strauf, P. Michler, G. Bacher, and A. Forchel, Triggered polarization-correlated photon pairs from a single CdSe quantum dot, Appl. Phys. Lett. **83,** 1848 (2003).

[70] G. V. Astakhov, T. Kiessling, A. V. Platonov, T. Slobodskyy, S. Mahapatra, W. Ossau, G. Schmidt, K. Bruuner, and L. W. Molenkamp, Circular-to-Linear and Linear-to-Circular Conversion of Optical Polarization by Semiconductor Quantum Dots, Phys. Rev. Lett. **96,** 027402 (2006).

[71] R. I. Dzhioev, B. P. Zakharchenya, E. L. Ivchenko, V. L. Korenev, Y. G. Kusraev, N. N. Ledentsov, V. M. Ustinov, A. E. Zhukov, and A. F. Tsatsulnikov, Optical orientation and alignment of excitons in quantum dots, Phys. Solid State **40,** 790 (1998).